Article ID: 1006-8775(2002) 02-0132-09

COUPLING PATTERNS OF AIR-SEA INTERACTION AT MIDDLE & LOWER LATITUDES AND THEIR INTERDECADAL OSCILLATION

ZHU Yan-feng (朱艳峰)[1], DING Yu-guo (丁裕国)[2], HE Jin-hai (何金海)[2]

(1. *LASG, Institute of Atmospheric Physics, Chinese Academy of Science, Beijing*, 100029 *China*; 2. *Nanjing Institute of Meteorology, Nanjing* 210044 *China*)

ABSTRACT: Diagnostic studies have been done of the seasonal and interdecadal variations of the coupling patterns for the air-sea interactions in the northern Pacific region, by using 500-hPa geopotential height field of the Northern Hemisphere and monthly mean SST field of northern Pacific Ocean (1951 ~ 1995) and with the aid of the Singular Value Decomposition (SVD) technique. The results show that: (1) The distribution patterns of SVD, which link with the El Niño (or La Niña) events, are important in the interaction between the atmosphere and ocean while the atmosphere, coupling with it, varies like the PNA teleconnection does. The coupling of air-sea interactions is the highest in the winter (January), specifically linking the El Niño event with the PNA pattern in the geopotential height field. Of the four seasons, summer has the poorest coupling when the 500-hPa geopotential height field corresponding to the La Niña event displays patterns similar to the East Asian-Pacific one (PJ). The spring and autumn are both transitional and the coupling is less tight in the autumn than in the spring. (2) Significant changes have taken place around 1976 in the pattern of air-sea coupling, with the year's winter having intensified PNA pattern of 500-hPa winter geopotential height field, deepened Aleutian low that moves southeast and the summer following it having outstanding PJ pattern of 500-hPa geopotential height field, which is not so before 1976.

Key words: air-sea interactions; coupling patterns; seasonal changes; interdecadal variation

CLC number: P732.6 **Document code:** A

1 INTRODUCTION

Large amount of work has been done and abundant results achieved in the relationship between teleconnections and ENSO and associated physical mechanisms since early 1980's. Both observational studies and numerical simulations have supported the argument that there is close linkage between wintertime Pacific SST and the Pacific-North America teleconnections (PNA) in the 500 hPa geopotential height field[1, 2]. As shown in Huang et al.[3] in their study of circulation anomalies for the boreal summer, there is what is called a pattern of East Asian-Pacific teleconnection, which is referred to as the Pacific-Japan Oscillation (PJ) by Nitta[4]. The meteorologist reports that the teleconnection wavetrain has close relationships with convection in the equatorial western Pacific and even the El Niño event. Teleconnection patterns allocate differently with SST in the winter and summer, suggesting significant seasonal variation in the coupling pattern of air-sea interactions.

Since the end of the 1980's, much research has been done on the abrupt climatic change that took place in mid-1970's. Trenberth[5] points out that beginning from 1976, decadal variations are obvious in the North Pacific circulation, which displays as the deepening and eastward movement of the Aleutian low in the wintertime troposphere and the ocean, like the atmosphere,

Received date: 2001-07-19; **revised date:** 2002-09-06
Foundation item: Research on the formation mechanism and prediction theories of major climatic calamities in China —a first initiated project in the Development Plan for National Key Fundamental Research; Natural Science Foundation of China (49575261); Natural Science Foundation of China (40023001)
Biography: ZHU Yan-feng (1970 –), female, native from Fujian Province, Ph.D., mainly undertaking the study of climatic change.

varies on the scale, too. With the EOF analysis, Nitta [7] argues that after 1976 there is a significant growing trend of the time coefficient for the first eigenvector of the global SST.

To summarize, we can see that the coupling pattern of air-sea interactions is subjected to both significant seasonal and interdecadal variations. Works that address them as a whole are few. It is therefore the aim of the current work to compare and study the coupling patterns of air-sea interactions over individual seasons and then to analyze the interdecadal variations of the patterns.

2 DATA AND METHODS

The current work uses the monthly mean 500-hPa data for the Northern Hemisphere at intervals of 10°×10° (provided by the National Meteorological Center of China), the monthly mean SST data at intervals of 7.5°×4.5° and over a domain of 22.5°N ~ 40.5° (provided by the ENSO center, Hawaii University). They both cover a period from January 1951 to December 1995.

Owing to its capability of taking into account mutual relationships in aspects of both time and space, the SVD method has been proved an efficient tool in studying patterns coupling any two element fields. It is why the work employs it in the study of the coupling patterns of air-sea interactions and the variation with time. According to the SVD theory [1, 8], the coupling signals extracted from the cross covariance matrix from two fields, denoted the left and right fields, are just the coupling modes constituted by a number of typical patterns of spatial distribution (of left and right singular vectors) and time series for corresponding expansion coefficients. The time-dependent variations of these modes are describable by means of the time series of their expansion coefficients. For example, the correlation coefficient between two components of time coefficients is indication of the correlation extent of the temporal variation of typical spatial distribution patterns that are extracted from the left and right fields. Known as the correlation coefficient of the mode, it is also measurable by the rate of contribution of the modes to the cross covariance matrix.

First of all, the covariance matrix X for SST and 500-hPa field is calculated. Then, SVD derivation is applied to X to obtain its singular values and singular vectors in the left and right fields. The two vectors correspond to spatial patterns for the SST and 500-hPa geopotential height field, respectively. To investigate into the coupling patterns of atmospheric and oceanic element fields, the time coefficients for the spatial patterns are determined and the simultaneous correlation between the coefficients for typical SST distribution and SST anomalies in the Pacific Ocean and between those for typical 500-hPa filed and 500-hPa geopotential height field in the Northern Hemisphere, are sought.

3 DATA ANALYSIS

3.1 *Seasonal variation of air-sea coupling patterns*

SVD is respectively applied to the fields of SST and geopotential height for January (standing for winter), April (spring), July (summer) and October (autumn). Tab.1 gives the percentage of contribution to the cross covariance matrix and to the left and right fields by the first pair of singular vectors so decomposed from the SST and geopotential height fields. The current work mainly studies the variation of the spatial distribution pattern for the first mode, because the variance percentage is large (more than 30.0%) for the spatial pattern of the first pair and able to describe major patterns of the air-sea coupling effect while the variance contribution for the remaining modes is only below 15%.

Tab.1 Summary of results for the first mode of SVD, based on the northern Pacific SST and 500-hPa geopotential height fields of January, April, July and October, respectively.

	January	April	July	October
Percentage for covariance / %	50.10	48.90	34.60	38.50
Correlation coefficients	0.85	0.89	0.79	0.78
Percentage for SST variance / %	20.00	17.10	14.50	20.60
Percentage for geopotential height field variance / %	13.60	13.10	11.20	9.30

Fig.1 presents the patterns of SST field and 500-hPa geopotential height field for the first pair of singular vectors. Panels on the left column are the SST patterns for January, April, July and October. From Fig.1a, we know that the eastern tropical Pacific is a region of positive correlation (as high as 0.8 at the center) and the westerly drift is a region of negative correlation. As shown in the variation of relevant time coefficient (the solid line), when it is at the peak (positive), the pattern of SST is positively anomalous over the equatorial eastern Pacific and the

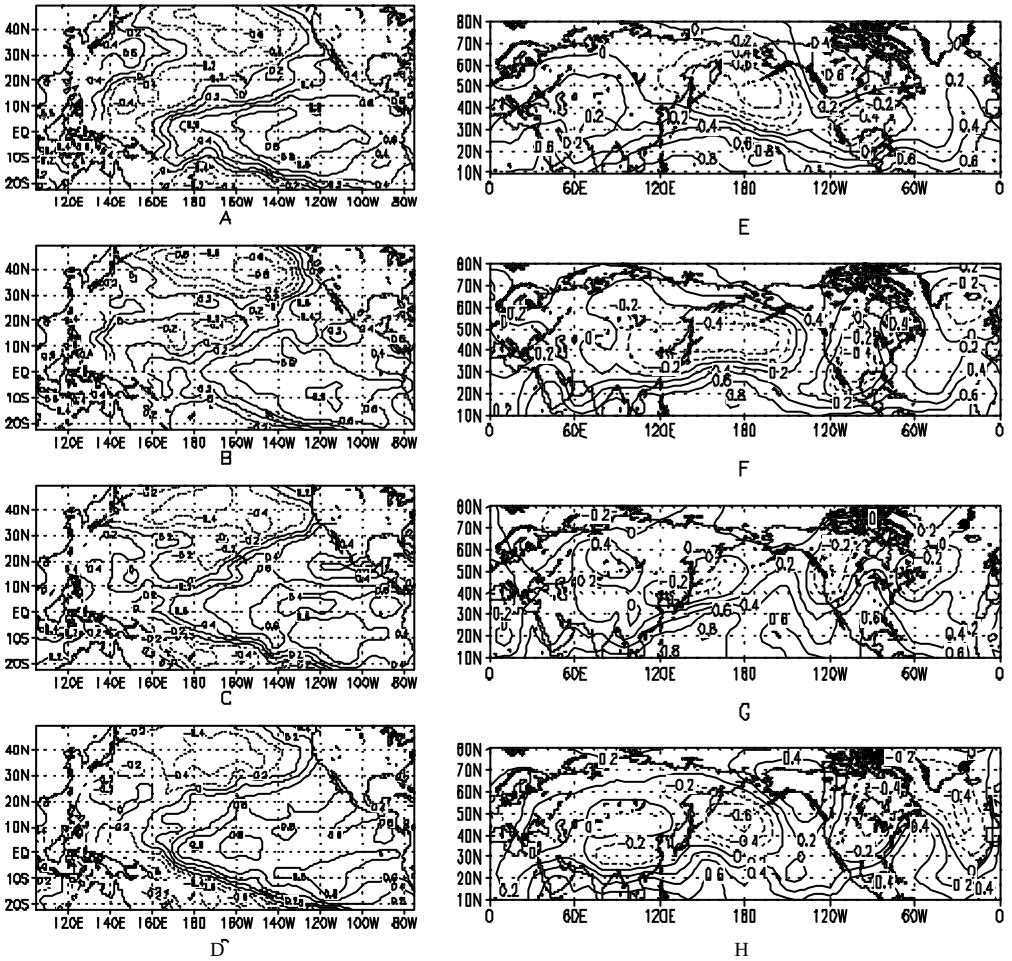

Fig.1 January, April, July and October patterns of geopotential height and SST fields for the first pair of singular vectors SVD-processed. Panels A ~ D are the SST patterns for January, April, July and October while Panels E ~ H are the geopotential patterns for the months, respectively.

kuroshio area but negatively anomalous over other waters. It is a typical pattern of SST distribution for the El Niño year —when it is at the bottom (positive), the SST pattern is just the opposite, being typical for the La Niña year. For the rest of the months, the SST is distributed like that in January (Fig.1b ~ d), being of either the El Niño or La Niña pattern. Likewise, we study the pattern of geopotential height field. As shown in Fig.1e, the first mode of the 500-hPa geopotential height field much resembles the PNA teleconnection pattern, further suggesting close relationship between the El Niño phenomenon and the PNA pattern. Compared with January, the spatial distribution pattern for April (Fig.1f) sees southward advancement of a negative correlation area formerly over the Aleutian Islands with the high-value sector extending to the Korean Peninsula, while a positive correlation area moves northwest from northwestern North America. When it comes to summer (July), the pattern (Fig.1g) shows that the correlation is positive around the region of the Philippines, Indochina Peninsula and southern China, negative from northern China to Japan, slightly positive over eastern Siberia and positive from Alaska to the Aleutian region. There are additional areas of negative and positive correlation respectively over the west coasts of the United States and Mexico. The structure, known as a "wavetrain", looks similar to the PJ teleconnection pattern[3, 4]. For October (Fig.1h), positive correlation is present at 500 hPa south of 25°N, with negative correlation over central and southern China and again over northern Pacific and southern part of the Aleutian Islands. In the meantime, the region from Alaska to northwestern Canada is positively correlated but the East Coast of the United States negatively correlated. By careful comparison of Figs.1e ~ 1h, we note that for every season the geopotential patterns are similar to the PNA teleconnection to some extent, only that the track of wavetrains vary depending on the change of season. For example, the wavetrain of July is more zonal than that of January, which may be caused by seasonal variation of basic flows in terms of location[9].

The air-sea coupling patterns for January, April, July and October (standing for winter, spring, summer and autumn, respectively) are studied. It is found that the SST pattern that is associated with the El Niño (or La Niña) event is playing an important role while the atmosphere coupled with it are showing variations similar to the PNA teleconnection pattern, when the atmosphere interacts with the ocean. The air-sea coupling is the highest in winter (January), showing specifically corresponding relationship between the El Niño event and the PNA pattern of geopotential height field. The summertime 500-hPa geopotential height field corresponding to La Niña is, in parallel, much like the East Asian ~ Pacific (PJ) pattern. Of the four seasons, the air-sea coupling is the poorest in summer while the autumn is less tightly coupled than the spring between the atmosphere and ocean, though they are both transitional.

3.2 *Interdecadal variation of air-sea coupling patterns*

Seasonal variations are discussed in the previous section. Over recent years, various works have reported significant interdecadal changes in both the ocean and atmosphere around the mid-and-late periods of the 1970's. Inevitably, the changes are reflected in the coupling pattern by which they interact with each other. Figs.2a ~ 2d give the temporal variation of time coefficient for the first pair of singular vectors SVD-processed from the geopotential and SST fields for these months. The solid line is the time coefficient of the SST field and the dashed line that of the geopotential height field, and portion of straight line denotes respectively the mean of time coefficients for two periods of 1951 ~ 1976 (Period 1) and 1977 ~ 1995 (Period 2). As shown in the figure, the mean for these two periods differs greatly. Fu et al[10]. draw a summary on the definition and detecting methods for abrupt climatic changes. The current work uses the smoothing *t*-test method to verify significant changes taking place in the mid-and-late stages of the 1970's. The result shows that significant changes did occur around 1976 in individual time coefficients, which pass the *t*-test with a significance level of 0.01. It suggests reflection of the

abrupt change in coupling pattern in every season regarding the air-sea interactions at the point of the 1970's.

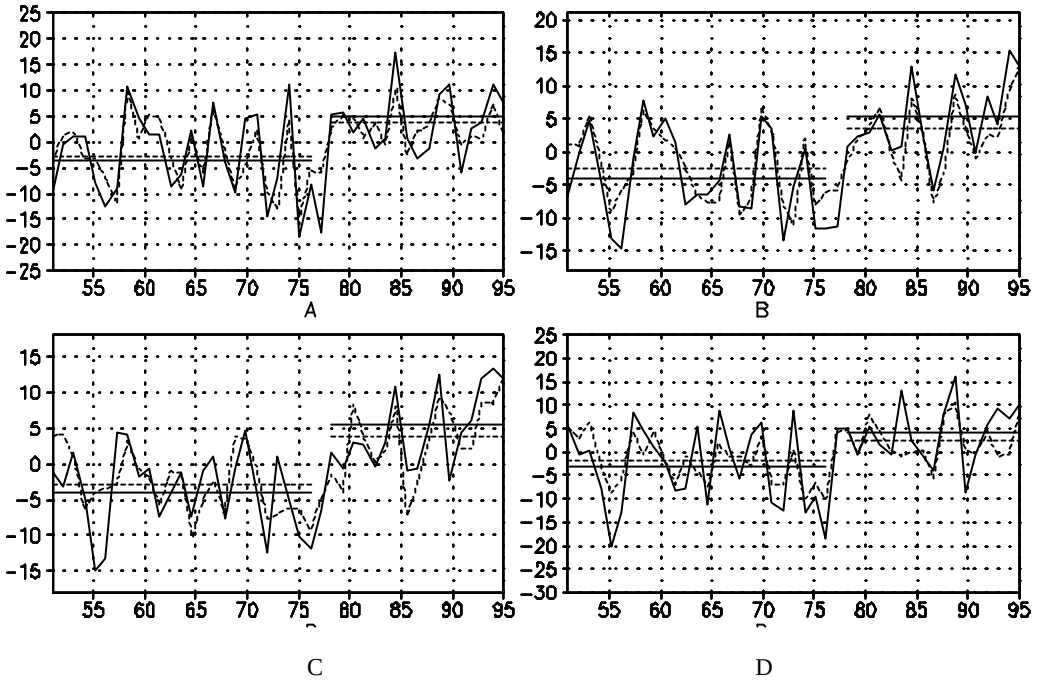

Fig.2 Temporal variation of time coefficients for the first mode SVD-processed of the geopotential height and SST fields in January, April, July and October. The solid line denotes the time coefficient of SST field and the dashed line that of geopotential height field.

In order to carry out the study, we must understand how climatic background changes for the coupling patterns. Difference charts for SST and 500-hPa geopotential height are drawn for January, April, July and October in Period 1 and Period 2, by subtracting Period 1 from Period 2. From Figs.3a ~ 3d, it is known that SST rises over tropical Pacific and North America coasts but falls over northern Pacific, with the largest amplitude in the central part of the latter region and the maximum drop of temperature more than –1.2℃ in July, the month of largest decrease. The change in SST fields has increased the north-south difference of SST. The SST field shows an increase in tropical central and eastern Pacific but decrease in the central part of northern Pacific, which is consistent with the El Niño distribution. Figs.3e ~ 3h are the difference in 500-hPa geopotential height by subtracting Period 1 from Period 2 for the four months. When we compare Figs.3e ~ 3h with Figs.1e ~ 1h, we find that they are quite similar in distribution pattern. Although there are significant changes around 1976 in the time coefficients for the first mode of either the SST or geopotential height field, as indicated in the study above, no similar changes have been found in the time coefficients for other modes. In summary, it can be inferred that the major change in general circulation at the point of the 1970's was taking place in the pattern of circulation for the first mode, i.e. it strengthens or weakens. For example, the North America high intensifies, the Aleutian low drops in pressure and pressure rises over the subtropics, in all months of January over Period 1, increasing the north-south pressure gradient and the speed of westerly wind. It is consistent with the variation of the SST field. Such coordinated action by the ocean and atmosphere on the interdecadal scale is resulted from long-term interactions.

The change in the atmosphere and ocean in the mid-and-late 1970's is closely related, as indicated above. It is mainly in the pattern of the first mode of the SST and geopotential height

fields (i.e. the first pair of eigenvectors after SVD) that the change materializes (by showing increased pattern for Period 2). To study the variation of the coupling pattern around 1976, singular vector decomposition is carried out for the SST and geopotential height fields over the two periods. Fig.4 shows the January patterns of distribution for the first pair singular vectors SVD-processed over the periods. Comparing the figures, we find changes in location in the 500-hPa teleconnection wavetrain for Period 2 (after 1976) and the high correlation center formally over the Aleutian region has displaced southeastward, suggesting displacement of the Aleutian low at the same direction over the period. It is consistent with the conclusion by Trenberth[5]. Similar significant changes are not found in the distribution pattern of SST field. Zhang[6] gives two modes of "horseshoes" and "saddles" for the interannual variation in tropical Pacific, with the former dominating before the 1990's and the latter playing a major role after it. As the current work focuses on the variations of coupling modes around the year 1976, which covers periods 1951 ~ 1976 and 1977 ~ 1995, the "horseshoes" become the principal pattern of SST.

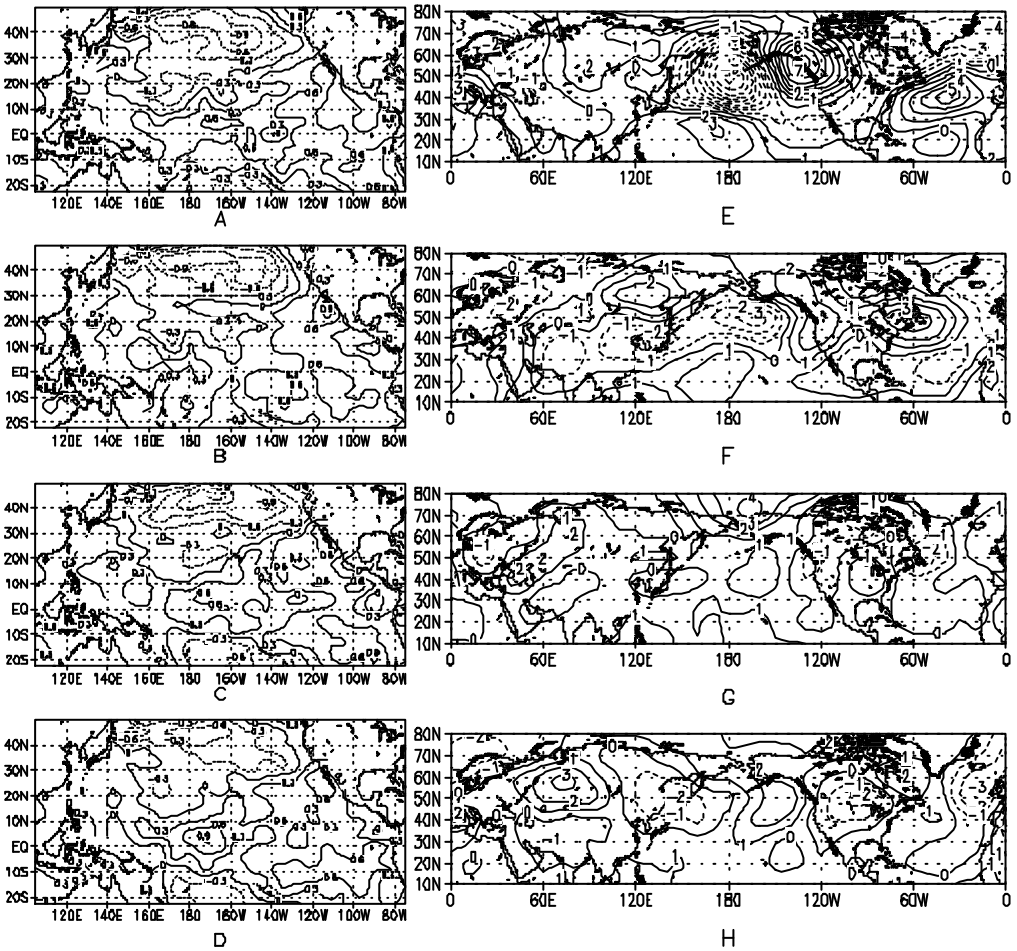

Fig.3 Difference in SST and 500-hPa geopotential height by subtracting Period 1 (1951 ~ 1976) from Period 2 (1977 ~ 1995) for January, April, July and October.

Fig.5 shows the July patterns of distribution for the first pair singular vectors SVD-processed for the SST and geopotential height fields over the periods. As shown in the figure, the patterns for both fields differ much between the two periods. The distribution of SST field for the second

period is consistent with the El Niño pattern while difference is large in the wavetrain structure between the periods as far as the 500-hPa geopotential height field is concerned. The wavetrain for Period 2 displays a pattern similar to the PJ teleconnection wavetrain put forward by Nitta[4] (Fig.5a) while that for Period 1 is not significant (Fig.5b). It may attribute to strengthened convection over tropical western Pacific after mid-1978. In fact, it was with the satellite data obtained after 1978 that Nitta and Huang Rong-hui suggested the presence of the PJ wavetrain.

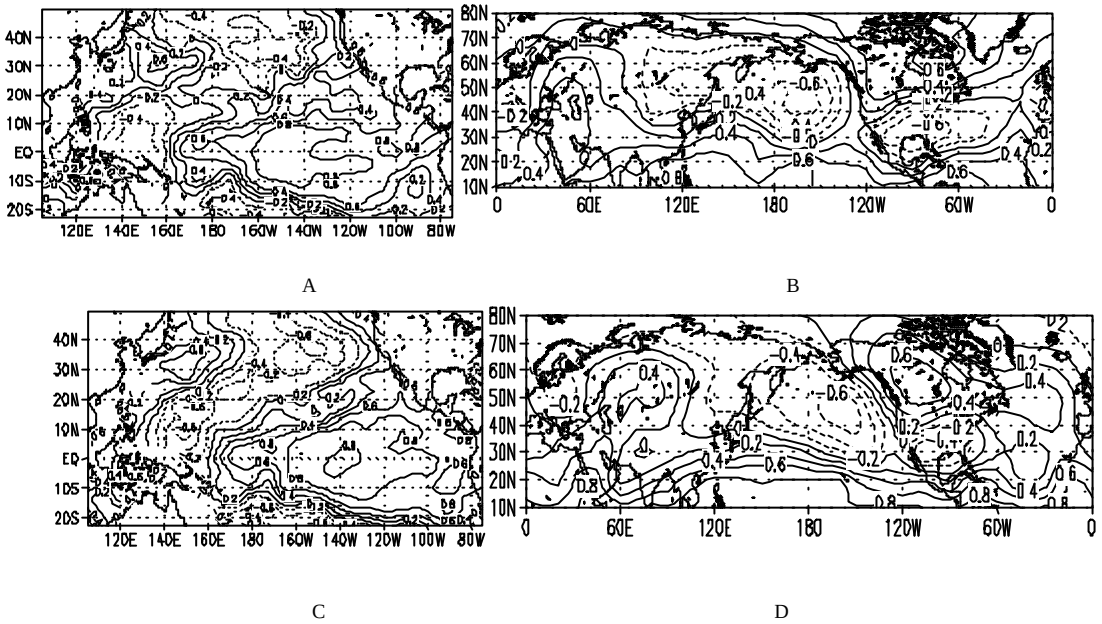

Fig.4 Distribution patterns of the first pair of eigenvectors SVD-processes for the January SST and geopotential height fields over Periods 1 and Periods 2. A and C are the patterns for the SST field over Period 1 and 2, respectively and B and D for the geopotential height field over Period 1 and 2, respectively.

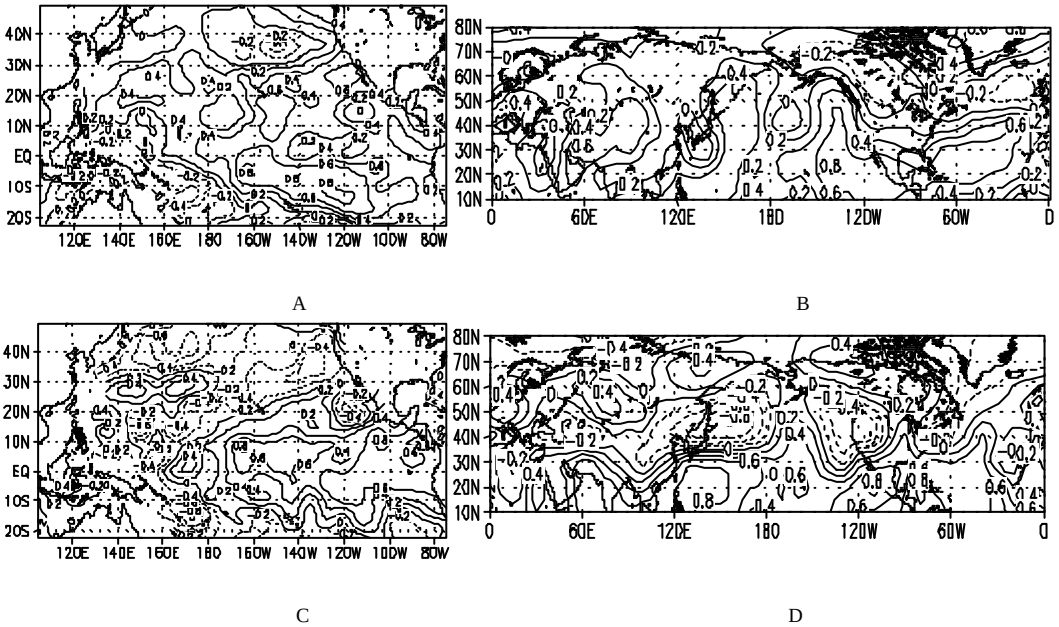

Fig.5 Same as Fig.4 but for July.

It is known from the study above that it has become warmer in tropical central and eastern Pacific but cooler in the central part of northern Pacific since mid-1970's, increasing the north-south contrast of SST. The significant changes in the climatic background of SST and geopotential height fields are reflected accordingly in their coupling pattern, particularly so in the SST field. Specifically, the PNA pattern increases in the wintertime 500-hPa geopotential height field, the Aleutian low deepens and moves southeast and the PJ pattern shows obviously in the summertime 500-hPa geopotential height field, which was not the case before 1976. In recent years, much modeling analysis has been performed in the aspect of interdecadal variation of the air-sea interactions, like Graham[11] and Miller[12] et al., but the results are useful in only describing the response of one member in the climate system to another, rather than explaining the causes and mechanisms responsible for the formation of interdecadal climatic variability. In their analysis of the relationship between climate change in China's summer (which is a season of frequent climate-inflicted disasters) and the anomalies of general circulation, Nitta et al.[13] point out that the air temperature over the middle and lower reaches of River Yangtze (Changjiang) varies with precipitation and the PJ wavetrain. It is presented in this work that the PJ wavetrain shows dominantly after the middle phase of the 1970's. These observational facts are helpful in making more study of the teleconnection mechanism for the air-sea interactions and more probes into any links between them and the variation of East Asian climate.

4 CONCLUDING REMARKS

a. During the interaction between the atmosphere and ocean, the SST patterns associating with the El Niño (or La Niña) events are playing an important role while the atmosphere coupled with them is showing changes similar to the PNA teleconnection pattern. The coupling of the air-sea interactions is the highest in winter (January), showing that El Niño event is responding to the PNA pattern in the geopotential height field while the summertime 500-hPa geopotential height field for the La Niña event look like the East Asian ~ Pacific (PJ) pattern. Of the four seasons, the air-sea coupling is the poorest in summer while the autumn is less tightly coupled than the spring between the atmosphere and ocean, though they are both transitional.

b. In addition to seasonal variation, the teleconnection pattern of the air-sea coupling is also characteristic of the obvious interdecadal one, with the changes in the SST and geopotential height fields taking place mainly in the pattern for the first mode (i.e. the first eigenvector pair SVD-processes), particularly so in the geopotential height field. Specifically, the PNA pattern increases in the wintertime 500-hPa geopotential height field, the Aleutian low deepens and moves southeast and the PJ pattern shows obviously in the summertime 500-hPa geopotential height field, which was not the case before 1976.

In this work, diagnostic analysis has been done of the coupling patterns of air-sea interactions and the interannual oscillations over northern Pacific region, with some interesting facts found. Physical mechanisms therein and possible linkage with the global climatic variation remain to be studied further.

Acknowledgements: Mr. CAO Chao-xiong, who works at the Guangzhou Institute of Tropical and Oceanic Meteorology, China Meteorological Administration, has translated the paper into English.

REFERENCES:

[1] WALLACE J M, SMITH C, BRETHERTON C S. Singular value decomposition of wintertime sea surface temperature and 500 hPa anomalies [J]. *Journal of Climate*, 1992, **5**: 561-576.

[2] LAU N C, NATH M J. A modeling study of the relative roles of the tropical and extra tropical SST anomalies in the variability of the global atmosphere-ocean system [J]. *Journal of Climate*, 1994, **7**: 1184-1207.

[3] HUANG Rong-hui, LI Wei-jing. Effect of heat source anomalies over tropical Pacific in summer on the

subtropical high over East Asia and its physical mechanism [J]. *Chinese Journal of Atmospheric Sciences* (formerly *Scientia Atmospherica Sinica*), 1988 (Special issue), 107-116.
[4] NITTA T. Convective activities in the tropical Western Pacific and their impact on the Northern Hemisphere summer circulation [J]. *Journal of Meteorological Society of Japan*, 1987, **65**: 373-390.
[5] TRENBERTH K E. Recent observal interdecadal climate change in the Northern Hemisphere[J]. *Bulletin of Atmospheric Society.* 1990, **71**: 988-993.
[6] ZHANG Qin. On the relationship between the anomalous development of ENSO in the 1990's and interdecadal climati change [D]. Beijing: Chinese Academy of Meteorological Sciences, 1999.
[7] NITTA T,YANMADA S. Recent warming of the tropical sea surface temperature and its relationship to the Northern Hemisphere circulation [J]. *Journal of Meteorological Society of Japan*. 1989, **67**: 375-383.
[8] DING Yu-guo, JIANG Zhi-hong. Generality of singular value decompositon in diagnostic analysis of meteorological field [J]. *Acta Meteorologica Sinica*, 1996, **54**: 365-372.
[9] LAU K M, PENG L. Dynamics of atmospheric teleconnections during the nor-thern summer[J]. *Journal of Climate*, 1992, **5**: 142-158.
[10] FU Zong-bin, WANG Qiang. The definition and detection of the abrupt climatic change [J]. *Chinese Journal of Atmospheric Sciences*, 1992, **18**: 482-493.
[11] GRAHAM N E. Decadal-scale climate variability in the tropical and North Pacific during the 1970s and 1980s: observations and model results [J]. *Climate Dynamics*, 1994, **10**: 135-162.
[12] MILLER A J. CAYAN D R, BARNETT T P, et al. Interdecadal variability of the Pacific Ocean: model response to observed heat flux and wind stress anomalies [J]. *Climate Dynamics*, 1994, **10**: 287-302.
[13] NITTA T, HU Zhen-zheng. Summer climate variability in China and its association with 500 hPa height and tropical convection [J]. *Journal of Meteorological Society of Japan*, 1996, **74**: 425-445.